Journal of Applied Mechanics and Technical Physics, Vol. 47, No. 3, pp. 455–460, 2006

CONTACT HOLOGRAPHIC INTERFEROMETER FOR STUDYING THE DEFORMATION OF SMALL-CURVATURE SHELLS OF REVOLUTION

S. I. Gerasimov[1] **and V. A. Zhilkin**[2]

UDC 535.317.1

The strains of a curvilinear surface are determined using holographic interferometry. Equations are derived to interpret the interference fringes for a shell of revolution.

Key words: *holographic interferometry, shell of revolution, surface-strain measurement.*

INTRODUCTION

Experimental optical methods are used to analyze the strain state of thin-wall structures of considerable area. However, existing methods have certain drawbacks, such as low sensitivity in the moire fringe method [1] and the dependence of the strain state of an article on the mechanical and elastic characteristics of the transducer in the photoelastic coating method [2]. In recent years, attempts have been undertaken to solve these problems using advanced high-sensitivity optical methods based on holographic techniques of information recording [3]. Unlike the classical methods, holographic methods allow one to compensate the optical aberration of the interferometer and to control the sensitivity to displacements during optical processing of holograms. A disadvantage of these methods is the need for vibration isolation of the employed experimental facilities, which hinders their use in factory laboratories. The requirements for the vibration isolation can be considerably lowered if the recording medium is fixed on the article tested [4, 5].

In the work described here, the deformation of shells of revolution were studied using an attached (contact) holographic interferometer [6].

1. EXPERIMENTAL TECHNIQUE

Interpretation of Holographic Interferograms. A plane monochromatic wave illuminates the surface being studied (Fig. 1). The illumination and observation directions are defined by the angles γ^{il} and γ^{ob}, respectively, which lie in the planes yOz (a plane case is considered). Only parallel light beams backscattered from the surface of the object are recorded.

During the first exposure, the optical path length of light $ABCDEFGH$ is given by

$$L_1 = \sum_{i=1}^{3} \frac{h_i n_i}{\cos \gamma_i^{\text{il}}} + \sum_{i=1}^{3} \frac{h_i n_i}{\cos \gamma_i^{\text{ob}}} + (V - W \tan \gamma_3^{\text{ob}}) \sin \gamma^{\text{ob}},$$

where h_i and n_i are thickness and the index of refraction of the ith layer ($i = 1, 2, 3$), V and W are the displacements of a point along the x and z coordinate axes, respectively, and γ_i are the angles of refraction of light in the ith layer.

[1]Siberian State University of Means of Communication, Novosibirsk 630049; gerasimov@stu.ru. [2]Chelyabinsk State Agroengineering University, Chelyabinsk 454080; vaz@mail.ru. Translated from Prikladnaya Mekhanika i Tekhnicheskaya Fizika, Vol. 47, No. 3, pp. 176–182, May–June, 2006. Original article submitted June 24, 2005.

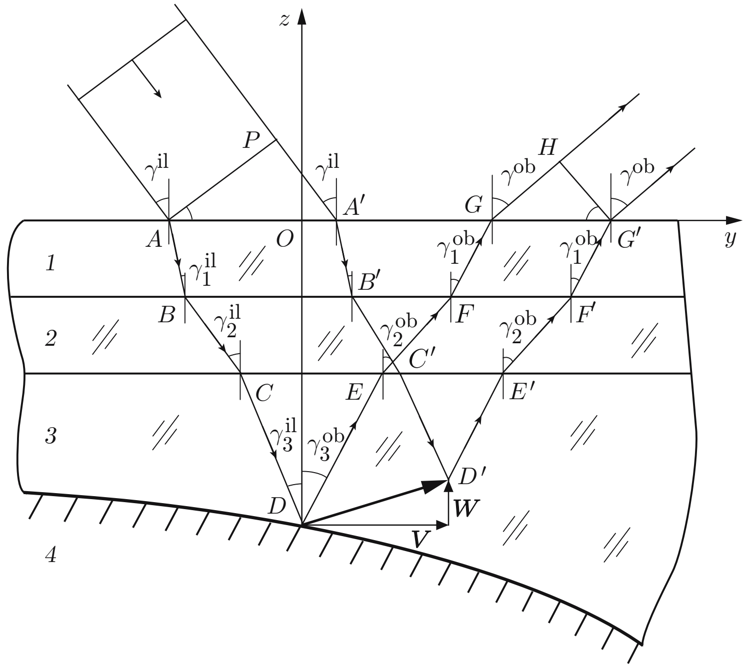

Fig. 1. Diagram of contact holographic interferometer: 1) holographic recording medium; 2) glass support; 3) air gap; 4) surface studied.

After the application of an external load to the shell, the point D moved to the point D'. In this case, the optical path length of the light beam is given by

$$L_2 = \sum_{i=1}^{3} \frac{h_i n_i}{\cos \gamma_i^{\text{il}}} + \sum_{i=1}^{3} \frac{h_i n_i}{\cos \gamma_i^{\text{ob}}} - W n_3 \Big(\frac{1}{\cos \gamma_3^{\text{il}}} + \frac{1}{\cos \gamma_3^{\text{ob}}} \Big) + (V + W \tan \gamma_3^{\text{il}}) \sin \gamma^{\text{il}}.$$

The light intensity in the interference pattern depends on the path difference $L = L_2 - L_1$.

The retrieved interference pattern is recorded in two directions in the plane yOz which are symmetric about the z axis to determine the components V and W separately. In this case,

$$V = \frac{(N_1 - N_2)\lambda}{2 \sin \gamma^{\text{ob}}};$$

$$W = \frac{(N_1 + N_2)\lambda}{2(\cos \gamma^{\text{il}} + \cos \gamma^{\text{ob}})} + \frac{(N_1 - N_2) \sin \gamma^{\text{il}} \lambda}{2(\cos \gamma^{\text{il}} + \cos \gamma^{\text{ob}}) \sin \gamma^{\text{ob}}}$$

$$= \frac{N_2 \lambda}{2(\cos \gamma^{\text{il}} + \cos \gamma^{\text{ob}})} \Big(- \frac{\sin \gamma^{\text{il}}}{\sin \gamma^{\text{ob}}} + 1 \Big) + \frac{N_1 \lambda}{2(\cos \gamma^{\text{il}} + \cos \gamma^{\text{ob}})} \Big(\frac{\sin \gamma^{\text{il}}}{\sin \gamma^{\text{ob}}} + 1 \Big). \quad (1)$$

Here $N_k(x, y) = 0, \pm 1, \pm 2, \ldots$ $(k = 1, 2)$ are the interference fringe numbers for the different observation directions and λ is the laser wavelength.

The component U $(k = 3, 4)$ is found similarly. Determining the displacements U, V, and W in the coordinate system (x, y, z) attached to the plane of the photoplate, it is necessary to convert to the components U^*, V^*, and W^* in a moving coordinate system that follows the shape of the surface. For this, we consider the general case of a shell of revolution (Fig. 2). The unit vectors $\boldsymbol{e}_x$, $\boldsymbol{e}_y$, and $\boldsymbol{e}_z$ of the moving coordinate system are expressed in terms of the fixed unit vectors $\boldsymbol{i}$, $\boldsymbol{j}$, and $\boldsymbol{k}$ as follows:

$$\boldsymbol{e}_x = \sin\theta \cdot \boldsymbol{i} + \cos\theta \sin\varphi \cdot \boldsymbol{j} + \cos\theta \cos\varphi \cdot \boldsymbol{k},$$

$$\boldsymbol{e}_y = 0 + \cos\varphi \cdot \boldsymbol{j} - \sin\varphi \cdot \boldsymbol{k},$$

$$\boldsymbol{e}_z = -\cos\theta \cdot \boldsymbol{i} + \sin\theta \sin\varphi \cdot \boldsymbol{j} + \sin\theta \cos\varphi \cdot \boldsymbol{k}$$

(θ and φ are the coordinate angles for the point considered).

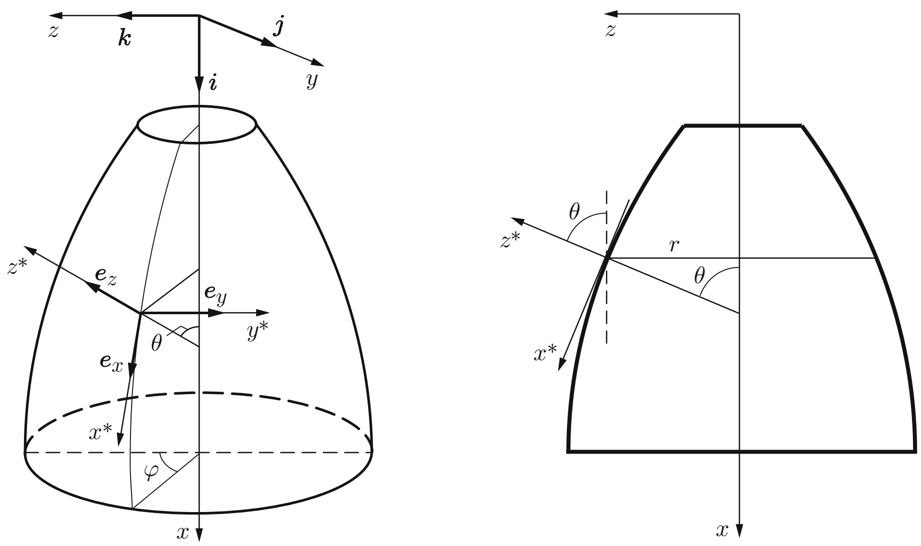

Fig. 2. Elements of the geometry of the shells of revolution.

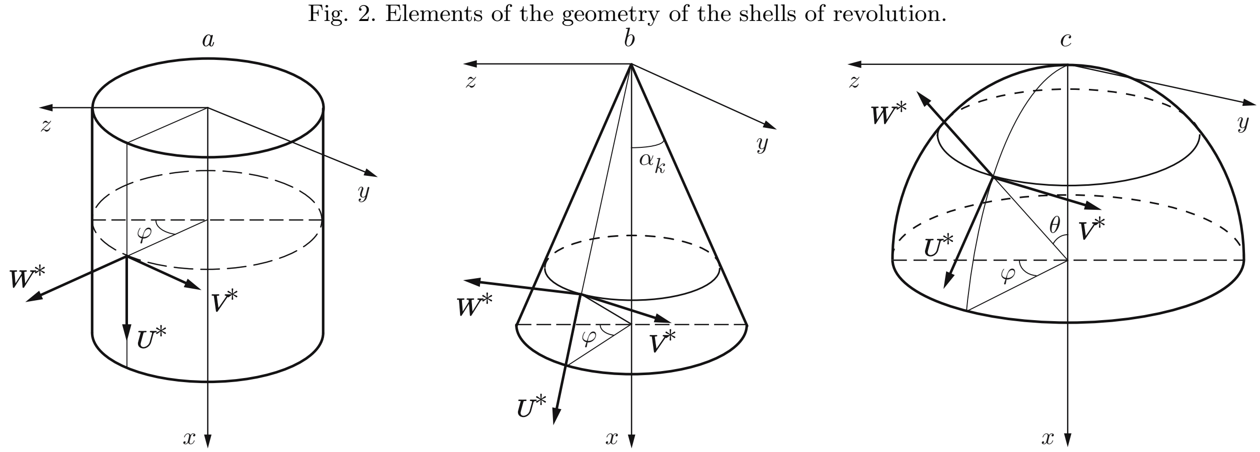

Fig. 3. Particular cases of shells of revolution: cylinder (a), cone (b), and sphere (c).

Below, we assume that the normal of the photoplate coincides with the z axis and the components U, V, and W need to be determined at the point of the surface to which the moving coordinate system (x^*, y^*, z^*) corresponds. If the direction cosines are known, the displacements for the three particular cases are defined as follows:

1) for a circular cylinder (Fig. 3a),

$$\begin{aligned} U^* &= U, \\ V^* &= V\cos\varphi - W\sin\varphi, \\ W^* &= V\sin\varphi + W\cos\varphi; \end{aligned}$$

2) for a circular cone (Fig. 3b),

$$\begin{aligned} U^* &= U\cos\alpha + V\sin\alpha\sin\varphi + W\cos\varphi\sin\alpha, \\ V^* &= V\cos\varphi + W\sin\varphi, \\ W^* &= -U\sin\alpha + V\cos\alpha\sin\varphi + W\cos\alpha\cos\varphi; \end{aligned}$$

3) for a sphere (Fig. 3c),

$$\begin{aligned} U^* &= U\sin\theta + V\cos\theta\sin\varphi + W\cos\theta\cos\varphi, \\ V^* &= V\cos\varphi + W\sin\varphi, \\ W^* &= -U\cos\theta + V\sin\theta\sin\varphi + W\sin\theta\cos\varphi. \end{aligned}$$

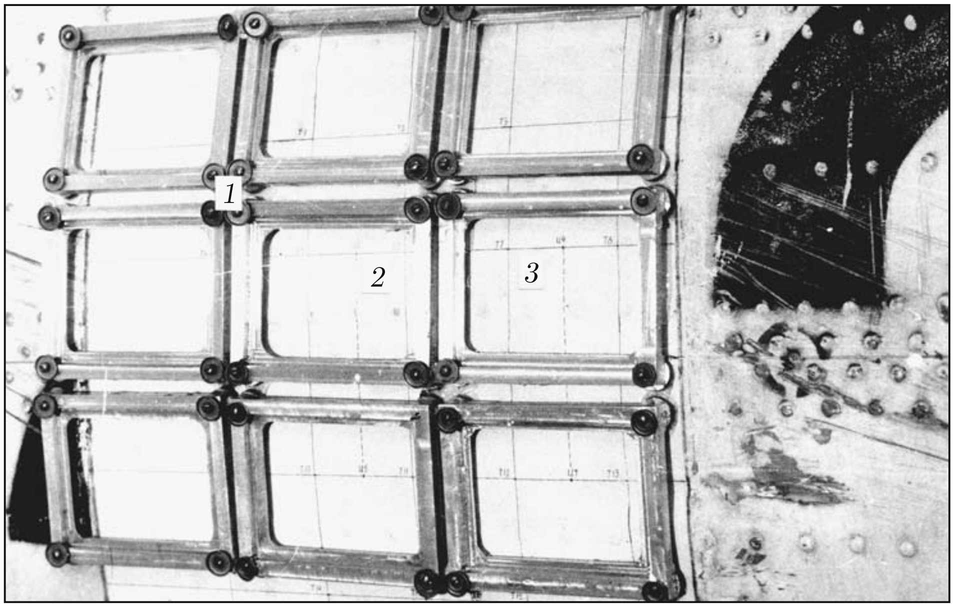

Fig. 4. Structure of mosaic interferometer: 1) photoplate holders; 2) point of application of the compressing force; 3) coordinate grid.

Calculation of Surface Strains. The strains of the middle surface of the shell of revolution are described by six components [7]:

$$\varepsilon_\theta = \frac{1}{R}\Big(\frac{\partial U}{\partial \theta} + W\Big), \qquad \varepsilon_\varphi = \frac{1}{R_\varphi \sin\theta}\Big(\frac{\partial V}{\partial \varphi} + U\cos\theta + W\sin\theta\Big),$$

$$\gamma = \frac{1}{R_\theta}\,\frac{\partial V}{\partial \theta} - \frac{\cos\theta}{R_\varphi \sin\theta}V - \frac{1}{R_\varphi \sin\theta}\,\frac{\partial U}{\partial \varphi}, \qquad \chi_\theta = -\frac{1}{R_\theta}\,\frac{\partial}{\partial \theta}\Big[\frac{1}{R_\theta}\Big(\frac{\partial W}{\partial \theta} - U\Big)\Big],$$

$$\chi_\varphi = -\frac{1}{(R_\varphi \sin\theta)^2}\Big(\frac{\partial^2 W}{\partial \varphi^2} - \sin\theta\,\frac{\partial V}{\partial \varphi}\Big) - \frac{\cos\theta}{R_\theta R_\varphi \sin\theta}\Big(\frac{\partial W}{\partial \theta} - U\Big), \tag{2}$$

$$\tau = -\frac{1}{R_\theta}\,\frac{\partial}{\partial \theta}\Big[\frac{1}{R_\varphi \sin\theta}\Big(\frac{\partial W}{\partial \varphi} - V\sin\theta\Big)\Big] + \frac{1}{R_\theta R_\varphi \sin\theta}\Big(\frac{\partial U}{\partial \varphi} - V\cos\theta\Big).$$

Expressions (2) contain the absolute values of U, V, and W, and a contact holographic interferometer is capable of recording only relative displacements (in the coordinate system of the photoplate). In this connection, it is necessary to make additional direct measurements of the indicated components at the outer edge of the interferometer (using, for example, an indicating gauge), and then to take them into account in constructing fields of $U(x,y)$, $V(x,y)$, and $W(x,y)$.

2. RESULTS OF EXPERIMENT

The object of research was a shell in the form of a truncated cone 120 cm high with a radius of the base of 85 cm and a slope angle of the generatrix of $2.5°$. On the inner surface of the shell there were periodically located stiffening ribs. Since the area of the region studied exceeded 1000 cm^2, a compound (mosaic) interferometer (Fig. 4) was used. Loading was implemented through a stringer by a point force P. The displacements W of the points of the shell surface were measured by indicating gauges, and the strain level on its inner surface was determined by KF-5R4 strain gauges.

Holograms were recorded using a two-exposure method. The pattern of fringes W recorded by the central photoplate (see Fig. 4) is given in Fig. 5. The hologram was interpreted with the use of formula (1) taking into account that the condition $\gamma^{\rm ob} = \gamma^{\rm il} = 0$ was satisfied in the experiment. Diagrams of $N(x,y)$ were plotted along

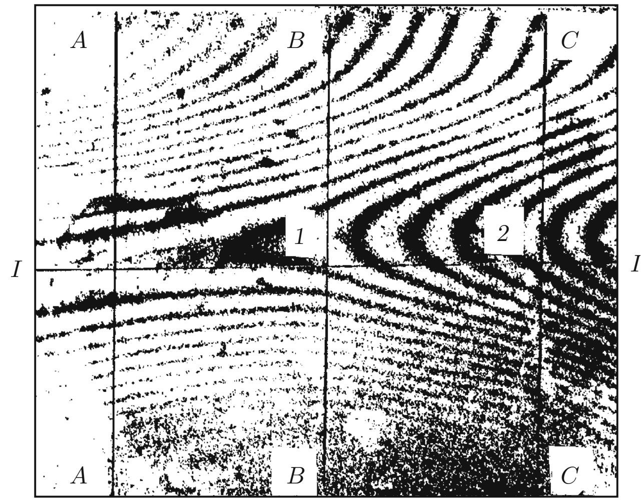

Fig. 5. Interferogram obtained for a compressing force $P = 50$ N.

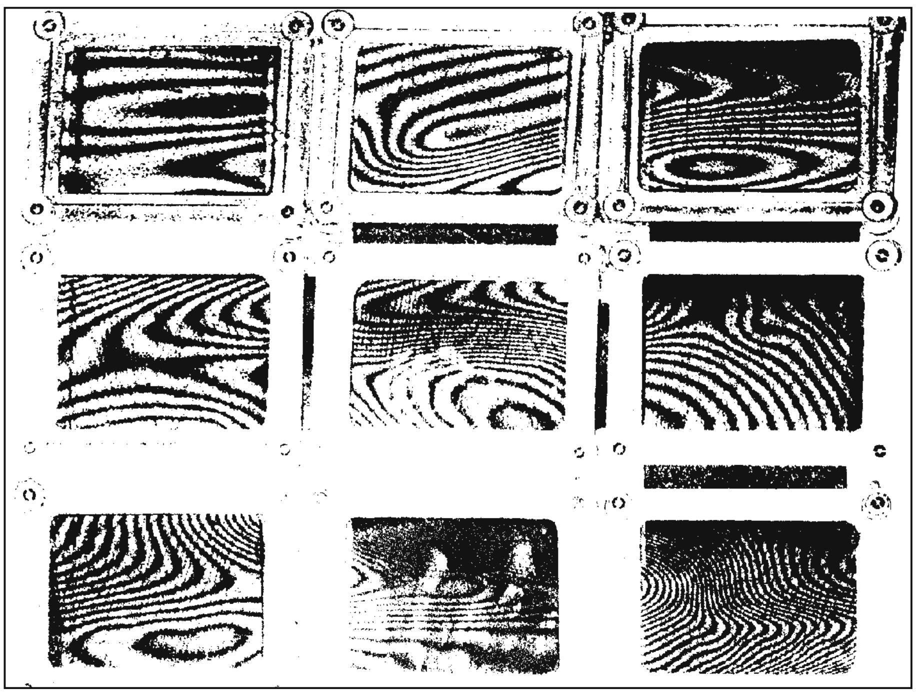

Fig. 6. Interferograms of a segment of the shell surface for $P = 40$ N.

the sections I–I, A–A, B–B, and C–C, local parabolic approximation of the function $N(x, y)$ was performed at the nodes of a nonuniform grid using the special USMI53 program, and the derivatives $\partial^2 W/\partial x^2$ and $\partial^2 W/\partial y^2$ were calculated. The USMI55 program provided a linear combination of fields of $N(x, y)$ for various observation directions [8].

For the shell studied, the ratio of the linear dimensions of one hologram to the curvature radius was such that, to a first approximation, the following relation corresponding to the hypothesis of straight normals could be considered valid:

$$\varepsilon_x = -z\Big(\frac{\partial^2 W}{\partial x^2} + \nu\,\frac{\partial^2 W}{\partial y^2}\Big), \qquad \varepsilon_y = -z\Big(\frac{\partial^2 W}{\partial y^2} + \nu\,\frac{\partial^2 W}{\partial x^2}\Big).$$

Here ε_x and ε_y are the strains of the shell surface, $z = h/2$ is the distance from a given point up to the middle plane, h is the shell thickness, and ν is Poisson's constant.

TABLE 1

Point in a Fig. 5	The value of ε_x	
	data of holography	data of strain measurements
1	$1.90 \cdot 10^{-5}$	$2.32 \cdot 10^{-5}$
2	$0.96 \cdot 10^{-5}$	$1.16 \cdot 10^{-5}$

The values of ε_x obtained for points 1 and 2 (see Fig. 5) are given in Table 1. The difference between the results obtained using holography and strain measurements is approximately 20%.

The interference patterns obtained for a load $P = 40$ N are given in Fig. 6. The arrangement of the photoplates is same as in Fig. 4.

CONCLUSIONS

The feasibility of testing shells of small curvature using holographic interferometry was confirmed experimentally for the first time. The resulting equations were obtained for the displacement vector components of points of the surface studied in moving and fixed coordinate systems. The results of processing of interference patterns and strain measurements are compared.

REFERENCES

1. A. J. Durelli and V. J. Parks, *Moire Analysis of Strain*, Prentice-Hall, Inc., Englewood Cliffs (1970).
2. A. Ya. Aleksandrov and M. Kh. Akhmetzyanov, *Polarization-Optical Methods of Solid Body Mechanics* [in Russian], Nauka, Moscow (1973).
3. Yu. I. Ostrovskii, V. P. Shchepinov, and V. V. Yakovlev, *Holographic Interference Methods of Strain Measurement* [in Russian], Nauka, Moscow (1988).
4. D. Post, B. Han, and P. Ifju, *High-Sensitivity Moire: Experimental Analysis for Mechanics and Materials*, Springer-Verlag, New York (1997).
5. D. B. Neumann and R. C. Penn, "Object motion compensation using reflection holography," *J. Opt. Soc. Amer.*, **62**, No. 12, 1373 (1972).
6. V. A. Zhilkin and S. I. Gerasimov, "Possibility of studying the strain state of articles using an attached interferometer," *Zh. Tekh. Fiz.*, **52**, No. 10, 2079–2085 (1982).
7. I. A. Birger (ed.), *Strength, Stability, Oscillations: Handbook* [in Russian], Vol. 1, Mashinostroenie, Moscow (1968).
8. A. P. Ustimenko, "Numerical study of the error of algorithms for processing experimental data," in: *Commercial Applications of Lasers* [in Russian], Ural. Dom Nauch.-Tekh. Propagandy, Chelyabinsk (1989), p. 43.